Solid Earth Discuss., 6, 1863–1905, 2014
www.solid-earth-discuss.net/6/1863/2014/
doi:10.5194/sed-6-1863-2014

Solid Earth
Discussions
Open Access

The diverse crustal structure and magmatic evolution of the Manihiki Plateau, central Pacific

K. Hochmuth[1], **K. Gohl**[1], **G. Uenzelmann-Neben**[1], **and R. Werner**[2]

[1]Alfred-Wegener-Institut Helmholtz-Zentrum für Polar- und Meeresforschung, Am Alten Hafen 26, 27568 Bremerhaven, Germany
[2]GEOMAR Helmholtz-Zentrum für Ozeanforschung, Wischhofstr. 1–3, 24148 Kiel, Germany

Received: 7 July 2014 – Accepted: 10 July 2014 – Published: 25 July 2014

Correspondence to: K. Hochmuth (katharina.hochmuth@awi.de)

Published by Copernicus Publications on behalf of the European Geosciences Union.

Abstract

The Manihiki Plateau is a Large Igneous Province (LIP) in the central Pacific. It was emplaced as part of the "Super-LIP" Ontong Java Nui and experienced fragmentation into three sub-plateaus, possibly during the break-up of Ontong Java Nui. The Manihiki Plateau is presumably the centerpiece of this "Super-LIP" and its investigation can therefore decipher the break-up mechanisms as well as the evolution of the plateau after its initial emplacement. By analyzing two seismic refraction/wide-angle reflection profiles crossing the two largest sub-plateaus of the Manihiki Plateau, the High Plateau and the Western Plateaus, we give new insights into their crustal structure and magmatic evolution. The High Plateau shows a crustal structure of 20 km thickness and a seismic *P* wave velocity distribution, which is comparable to other LIPs. The High Plateau experienced a strong secondary volcanism, which can be seen in relicts of seamount chain volcanism. The Western Plateaus on the other hand show no extensive secondary volcanism and are mainly structured by fault systems and sedimentary basins. A constant decrease in Moho depth (9–17 km) is a further indicator of crustal stretching on the Western Plateaus. Those findings lead to the conclusion, that the two sub-plateaus of the Manihiki Plateau experienced a different magmatic and tectonic history. Whereas the High Plateau experienced a secondary volcanism, the Western Plateaus underwent crustal stretching during and after the break-up of Ontong Java Nui. This indicates, that the sub-plateaus of the Manihiki Plateau play an individual part in the break-up history of Ontong Java Nui.

1 Introduction

Large Igneous Provinces (LIP) are large ($> 0.1 \times 10^6$ km^2) marine and terrestrial areas overprinted by massive volcanic activity (Bryan and Ernst, 2008) LIPs have a great impact on the environment during and after their emplacement, for instance by the release of greenhouse gases during massive volcanism (Wignall, 2001) or their role

SED

6, 1863–1905, 2014

Diverse crustal structure and magmatic evolution of the Manihiki Plateau

K. Hochmuth et al.

in plate motion by thickening of oceanic crust (Bryan and Ernst, 2008; Miura et al., 2004). The emplacement of LIPs can for instance be linked to multiple global mass extinction events (Bryan and Ernst, 2008; Coffin et al., 2006; Courtillot et al., 1999; Larson and Erba, 1999; Tarduno, 1998; Wignall, 2001). LIPs are the result of massive volcanic eruptions occurring during a relatively short time (1–5 Myr) resulting in an anomalously thick oceanic crust (Bryan and Ernst, 2008; Wignall, 2001). This first volcanic stage of a LIP event is characterized by the emplacement of approximately 75 % of its igneous volume (Bryan and Ernst, 2008; Bryan and Ferrari, 2013; Karlstrom and Richards, 2011; Miura et al., 2004). Later volcanic stages can be summarized as secondary volcanism and show longer emplacement periods as well as smaller emplacement rates. The crustal structure of oceanic LIPs commonly consists of a lower crustal layer with high seismic *P* wave velocities, mafic intrusions in the middle crust, and volcanic flow units in the uppermost crust (Coffin et al., 2006; Ridley and Richards, 2010; Wignall, 2001). In previous publications, the formation of LIPs on continents and oceans was explained by the mantle plumes having an initial phase of a hot spot trail (Miura et al., 2004; White and McKenzie, 1995). But this scenario has been debated, since this plume head model cannot explain all characteristics of oceanic LIPs (Bryan and Ernst, 2008; Coffin et al., 2006, 2002; Courtillot et al., 1999; Korenaga, 2005; Larson and Erba, 1999; McNutt, 2006; Tarduno, 1998). The Manihiki Plateau, located in the western central Pacific, is such a LIP with atypical features such as a laterally heterogeneous crustal character.

In this paper, we try to unravel the relationship between the two largest sub-plateaus of the Manihiki Plateau, the Western Plateaus and the High Plateau, which are separated by the Danger Island Troughs. Did both sub-plateaus experience the same magmatic history? The fragmentation of the Manihiki Plateau poses the question, whether distinct phases of igneous or tectonic processes led to the break-up to the Manihiki Plateau and which role the Danger Island Troughs played in this scenario. By processing, modeling and interpreting recently acquired seismic refraction/wide-angle reflection data the deep crustal structure of both sub-plateaus is revealed and interpreted for the first time.

2 Geological background

The formation of the Manihiki Plateau took place during the early Cretaceous (123–120 Ma) as centerpiece of the "Super-LIP" Ontong Java Nui according to Taylor (2006) and Chandler et al. (2012, 2013). This giant LIP covered 0.8 % of Earth's surface (Bryan and Ernst, 2008; Coffin and Eldholm, 1993; Ingle and Coffin, 2004; Wignall, 2001) and consisted of the Ontong Java Plateau, the Hikurangi Plateau and the Manihiki Plateau (Fig. 1 (inlet)) as well as presumed multiple smaller fragments to the northeast and east of the Manihiki Plateau, which have possibly been subducted (Larson et al., 2002; Viso et al., 2005). The break-up of Ontong Java Nui took place shortly after its emplacement, since secondary volcanism, which can be related to later volcanic phases with smaller eruption rates and mainly seamount volcanism, shows different petrological and geochemical characteristics on the three remaining plateaus (Hoernle et al., 2010; Timm et al., 2011). This led to the conclusion, that after the coupled emplacement of the plateaus, the multiple stages of secondary volcanism were supplied by different mantle sources. Seafloor spreading was established possibly around 118 Ma in Ellice Basin (Ontong Java–Manihiki) (Chandler et al., 2012) and at the Osbourn Trough (Hikurangi–Manihiki) (Worthington et al., 2006). The onset and the duration of seafloor-spreading at both locations is difficult to date, since the complete activity of those spreading-centers has occurred within the Cretaceous Magnetic Quiet Period. Therefore, no magnetic seafloor-spreading anomalies can be traced, and smaller changes in the magnetic field cannot be observed due to the severe volcanic overprinting (Billen and Stock, 2000).

The Manihiki Plateau itself experienced fragmentation into three sub-plateaus, the High Plateau, the Western Plateaus and the North Plateau (Winterer et al., 1974) (Fig. 1). Further significant features of the Manihiki Plateau are the Danger Island

Troughs, which are a failed rift separating the High Plateau from the Western Plateaus (Clague, 1976), the Suvorov Through and the Manihiki Scarp, a former shearing zone at the eastern part of the plateau (Larson et al., 2002).

Hussong et al. (1979) published first estimates on the crustal structure of the Manihiki Plateau. However, their experiment, using seismic sonobuoy data, did not provide data of the lower crustal layers or the upper mantle, but it was inferred that the crust of the Manihiki Plateau was 3.1 times thicker than average oceanic crust and that it showed similar features as described for the crust of the Ontong Java Plateau (Hussong et al., 1979).

The upper basement and the sedimentary cover of the Manihiki Plateau has been studied from samples collected by multiple dredges (Ai et al., 2008; Beiersdorf et al., 1995a; Clague, 1976; Hoernle et al., 2010; Ingle et al., 2007; Schlanger et al., 1976; Timm et al., 2011; Werner et al., 2013) and short sediment cores. Drilling at Deep Sea Drilling Project (DSDP) Leg 33 Site 317 reached a basaltic layer in a depth of 910 m below seafloor (Schlanger et al., 1976). This basaltic layer and other $^{40}Ar/^{39}Ar$ dated tholeiitic basalts reveal basement ages of the High Plateau between 124.6 ± 1.5 Ma (Timm et al., 2011) and 122.9 ± 1.6 Ma (Hoernle et al., 2010). In the Danger Island Troughs, tholeiitic basalts ($^{40}Ar/^{39}Ar$ age of 117.9 ± 3.5 Ma) with an unusual composition are present, as well as alkali basalts possibly related to later volcanic stages ($^{40}Ar/^{39}Ar$ age of 99.5 ± 0.7 Ma) (Ingle et al., 2007).

This second stage of episodic volcanism on the Manihiki Plateau is also depicted by multiple seamounts on the High Plateau (Beiersdorf et al., 1995b; Coulbourn and Hill, 1991). Seismic reflection data image several volcaniclastic layers in the lower sedimentary column (Ai et al., 2008; Schlanger et al., 1976; Winterer et al., 1974), pointing to a shallow or subaerial environment during the secondary phases of volcanism (Ai et al., 2008). It is important to note, that most of the publications have focused on the High Plateau along with the Danger Island Troughs and the Manihiki Scarp. Other areas of the Manihiki Plateau, such as the Western Plateaus, are poorly sampled and therefore the evolution of the different sub-plateaus and their magmatic and tectonic relationship to the other parts of the plateau is still poorly understood. Although satellite-derived gravity anomaly maps (Sandwell and Smith, 1997) indicate different crustal structures of the sub-plateaus, plate tectonic reconstructions of Ontong Java Nui (Chandler et al., 2012, 2013; Taylor, 2006) treat the Manihiki Plateau as a single tectonic block and disregard its fragmentation.

3 Data acquisition, processing, and modeling parameterization

3.1 Data acquisition

During R/V *Sonne* cruise SO-224 in 2012 (Uenzelmann-Neben, 2012), the Alfred Wegener Institute (AWI) collected two deep crustal seismic refraction/wide-angle reflection lines (Fig. 1), crossing the two main sub-plateaus of the Manihiki Plateau: the Western Plateaus (AWI-20120100) and the High Plateau (AWI-20120200). Both seismic lines consisted of 28 ocean-bottom seismometer (OBS) and 5 ocean-bottom hydrophone (OBH) stations spread out over 500 km long profiles each. The OBS stations were equipped with a 3-component (4.5 s natural period) seismometer and a hydrophone. OBH stations are only equipped with a hydrophone. Station spacing varied between a constant 14.1 km on AWI-20120100 and 10.9 km to 24.1 km on AWI-20120200 to ensure better ray-coverage at the plateau margins.

An array of 8 G-Guns™ (type 520) with a total volume of 68 L (4160 in^3) was used as a seismic source. The G-Guns™ were towed in four clusters of two guns each at 10 m water-depth and fired at nominally 200 bar operating pressure every full minute. During the acquisition, multichannel seismic reflection data was also recorded with a 3000 m long digital solid streamer (Sercel Sentinel™) of 240 channels. In addition to the seismic experiments, multibeam bathymetry data were collected throughout the cruise with a *Kongsberg Simrad EM120*, which is permanently installed on R/V *Sonne*.

3.2 Processing and modeling of seismic refraction/wide-angle reflection data

The OBS/OBH field data were merged with navigation data and converted to SEGY-format. After relocalization of the OBS positions using the direct-wave arrivals, all refracted and reflected arrival phases were picked with the software *ZP* (Zelt, 2004). We assigned picking uncertainties to the individual picks taking the signal-to-noise-ratio into account.

P wave and S wave velocity-depth modeling was carried out using the forward modeling software *Rayinvr* (Zelt and Smith, 1992) and its graphical interface *P-Ray* (Fromm, 2012). We used bathymetric and seismic reflection records obtained during the cruise, in order to constrain modeling parameters for the seafloor and the thickness of the sedimentary cover. The layer boundaries and model coordinates of the velocity nodes established by the P wave model were used for S wave modeling to ensure comparable models and allow the calculation of the Poisson's ratio.

Refracted and reflected phases in the P and S wave models are named respectively to their corresponding layer P_{layer} and $P_{\text{layer}}P/S_{\text{layer}}$ and $S_{\text{layer}}S$. Reflected phases always represent the reflection at the base of the layer. Mantle phases are called P_n/S_n for the refracted phase and P_mP/S_mS for the reflection at the crust-mantle boundary (Moho). We observed three distinct groups of crustal phases ($P_{\text{uc}}/S_{\text{uc}}$ (upper crust), $P_{\text{mc}}/S_{\text{mc}}$ (middle crust), $P_{\text{lc}}/S_{\text{lc}}$ (lower crust)) on the Western Plateaus (Figs. 2 and 3), and four distinct groups of crustal phases ($P_{\text{uc}}/S_{\text{uc}}$ (upper crust), $P_{\text{umc}}/S_{\text{umc}}$ (upper-middle crust), $P_{\text{lmc}}/S_{\text{lmc}}$ (lower-middle crust), $P_{\text{lc}}/S_{\text{lc}}$ (lower crust)) on the High Plateau (Figs. 4 and 5). The resolution of the S wave velocity models is generally lower than the resolution of the presented P wave velocity models. Unfortunately, only little to no information on the S wave velocity distribution was returned from the lower crust and the mantle.

The Poisson's ratio can contribute further parameters on the composition of the crust (Christensen, 1996). For example, alteration processes such as serpentinization or the distribution of predominantly mafic and felsic rocks can be constrained. We calculated

SED
6, 1863–1905, 2014

the Poisson's ratio for every velocity node of the P and S wave models and gridded their distribution. Since the S wave model has a sparser resolution than the P wave model, it limits the resolution of the Poisson's ratio model.

3.3 Modeling of gravity data

As shipborne gravity data were not collected, we relied on free-air gravity anomaly records extracted from the global satellite-derived gravity anomaly grid by Sandwell and Smith (1997) with values extracted along our seismic profiles. In a starting model using the forward modeling software IGMAS, we incorporated the layer boundaries of the P wave velocity-depth model and converted the P wave velocities to rock densities using the relationship by Hamilton (1978). We assigned rock densities to P wave velocity clusters representing the different crustal layers of the P wave velocity models (Table 1). As this 2-D approach turned out to be affected by large-amplitude anomaly features offline, a perfect fit could not be achieved by retaining realistic model parameters. In several iterations, the model parameters were altered to generate a best fit to the observed the gravity anomalies and the P and S wave models.

4 The crustal structure of the Western Plateaus and the High Plateau of the Manihiki Plateau

4.1 Bathymetric and sedimentary features

The two seismic refraction/wide-angle reflection profiles allow a comparison of the two main plateaus of the Manihiki Plateau. Profile AWI-20120100 crosses the Western Plateaus from the northwest to the southeast (Fig. 1). The water depth ranges from 4800 m in the Tokelau Basin to 3800 m on the Western Plateaus. The deepest areas of the profile are the Danger Island Troughs with a maximum depth of 4900 m. A small part of the westernmost High Plateau is also covered at the eastern end of this profile. Bathymetric and seismic reflection data reveal a rough seafloor with multiple faults and graben systems. Sedimentary cover is mainly restricted to the basins between the numerous basement highs.

Profile AWI-20120200 images the High Plateau of the Manihiki Plateau in a west to east section (Fig. 1). The water depth ranges from 5100 m in the Samoan Basin and Penrhyn Basin to a mean depth of the High Plateau of 2500 m with a relatively smooth seafloor. The Manihiki Scarp in the east and the margin towards the Samoan Basin in the west form sharp flanks bordering the sub-plateau. Seismic reflection data reveal an approximately 800 m thick sedimentary cover and several basement highs on the central plateau. Sedimentation appears to be restricted to pockets and small basins between basement highs on the margins of the High Plateau.

4.2 Upper crustal layers

The upper crustal layer of the Western Plateaus and the High Plateau include the acoustic basement of the seismic reflection data and are represented by the refracted phases (P_{uc}/S_{uc}) and constrained by the wide-angle reflections at the upper layer boundary P_sP and $P_{uc}P$ at the base of the layer (Figs. 2–5).

On the Western Plateaus, the upper crust is characterized by a rough basement topography and a widely variable velocity field. The western 50 km of the profile consist of an upper crustal layer with P wave velocities between 5.2 and 5.5 km s^{-1} (Fig. 6). Between 50 km and 300 km profile distance, P wave velocities decrease down to 4.5 km s^{-1} with small patches of lower velocities (3.8 km s^{-1}). It is important to note that due to the malfunction of two neighboring stations (st19, st20) the ray coverage is not ideal in this area. Between 300 and 370 km profile distance, unusual low velocities ranging from 3.0 to 4.3 km s^{-1} are present. S wave velocities show a block-like structure (Fig. 7). From 0 to 100 km, S wave velocities range from 2.9 to 3.2 km s^{-1}. Velocities decrease to 2.5 to 2.8 km s^{-1} between st8 and st12. From 180 km to 250 km profile distance, S wave velocities from 2.9 to 3.3 km s^{-1} are common. This block is followed by an area of unusual high S wave velocities, which corresponds to higher velocities in the middle crust (3.7 to 4.3 km s^{-1}). The Danger Island Troughs area lacks a visible upper crust (Figs. 2b and 6).

The High Plateau shows higher and more homogenous P wave velocities between 4.7 and 5.6 km s^{-1} (Figs. 4 and 8) and S wave velocities between 2.7 and 3.2 km s^{-1} (Figs. 5 and 9). Several magmatic extrusive and intrusive features can be identified in the seismic reflection data (Pietsch and Uenzelmann-Neben, 2014). Those volcanic centers can be connected to areas of higher P wave velocities (e.g. at st21) in the P wave velocity model.

The upper crust of the surrounding ocean basins, the Penrhyn Basin and the Samoan Basin show P wave velocities between 5.2 and 5.8 km s^{-1} (Fig. 8). S wave velocities range from 3.3 km s^{-1} in the Samoan Basin to 2.9 km s^{-1} in the Penrhyn Basin (Fig. 9). Whereas the Samoan Basin shows Poisson's ratio values of around 0.25, which can be related to basalt (Christensen, 1996), the Penrhyn Basin on the other hand shows high Poisson's ratio values of over 0.30 (Fig. 10). Those values are typical for serpentinized crust (Christensen, 1996).

4.3 Middle crustal layers

The middle crustal layers of the Manihiki Plateau consist of two layers ($P_{\mathrm{umc}}/S_{\mathrm{umc}}$ from upper-middle crust and $P_{\mathrm{lmc}}/S_{\mathrm{lmc}}$ from lower-middle crust) on the High Plateau and one layer on the Western Plateaus ($P_{\mathrm{mc}}/S_{\mathrm{mc}}$) (Figs. 2–5). On the Western Plateaus, the P wave velocity structure of the middle crust is homogeneous and ranges between 5.8 and 6.8 km s^{-1} (Fig. 6). In between the ridge-like structures at 230 and 270 km profile distance, the middle crustal layer extends to the basement. This feature is also present in the gravity anomaly model (Fig. 11). The S wave velocity model shows more variation in the middle crust, with values ranging from 3.6 to 4.0 km s^{-1} in the west to very high S wave velocities of up to 4.3 km s^{-1} at st22 (Fig. 7). S wave velocities decrease to 3.8 to 4.0 km s^{-1} towards the Danger Island Troughs.

Discussion Paper | Discussion Paper | Discussion Paper | Discussion Paper |

SED
6, 1863–1905, 2014

The middle crust is present at the Danger Island Troughs. East of the troughs, the middle crust is divided into two separate crustal layers, the upper-middle crust and the lower-middle crust (Figs. 4 and 6). The upper-middle crust shows *P* wave velocities between 5.4 and 6.4 $\mathrm{km\,s^{-1}}$ (Fig. 6) and *S* wave velocities between 3.0 and 3.6 $\mathrm{km\,s^{-1}}$ (Fig. 7). This crustal layer is thicker in the western part of the High Plateau. The lower-middle crust presents relatively high *P* wave velocities (6.7 to 6.9 $\mathrm{km\,s^{-1}}$) and *S* wave velocities between 4.0 and 4.3 $\mathrm{km\,s^{-1}}$ (Figs. 8 and 9). The lower-middle crustal layer crops out at the seafloor at the Manihiki Scarp. Here, *S* wave velocities up to 4.65 $\mathrm{km\,s^{-1}}$ are present. The Poisson's ratio shows three distinct areas of higher values (> 0.26) below the central plateau (Fig. 10). Those can be connected to areas of higher *P* wave velocities and therefore the volcanic structures within the upper crust. Middle crustal layers are not present in the adjacent oceanic basins.

4.4 Lower crustal layers

The lower crust of most Large Igneous Provinces consists of a zone of high *P* wave velocities ($> 7.1\,\mathrm{km\,s^{-1}}$), a so called high-velocity zone (HVZ) (Coffin et al., 2006; Ridley and Richards, 2010). On the Manihiki Plateau, we observe this HVZ on both sub-plateaus within the lower crust (P_{lc}/S_{lc}). *P* wave velocities range between 6.8 and 7.8 $\mathrm{km\,s^{-1}}$ on the Western Plateaus (Fig. 6) and 7.0 to 7.8 $\mathrm{km\,s^{-1}}$ on the High Plateau (Fig. 8). The ray-coverage of *S* waves is poor on the High Plateau and only very little interpretable signals were returned for the lower crust of the Western Plateaus. *S* wave velocities range between 4.1 and 4.3 $\mathrm{km\,s^{-1}}$ on the Western Plateaus (Fig. 7). At the western margin of the High Plateau, *S* wave velocities reach 4.4 $\mathrm{km\,s^{-1}}$ and at the Manihiki Scarp values of 4.7 $\mathrm{km\,s^{-1}}$ are present (Fig. 9).

4.5 Crust-mantle boundary and mantle

The boundary between the crystalline crust and the mantle (Moho) can be constrained by refracted phases from the uppermost mantle (P_n) as well as reflections at the Moho

SED
6, 1863–1905, 2014

itself (P_mP) (Figs. 2 and 4). On the High Plateau, the Moho is visible in the data throughout the central plateau at a depth of 20 km below the seafloor (Figs. 8 and 12). In the Samoan Basin and the Penrhyn Basin the crustal thickness, which includes the sedimentary cover, changes rather abruptly to only 5 km. Those depths for the crust-mantle boundary are also consistent with gravity anomaly modeling (Fig. 12). The uppermost mantle shows normal mantle P wave velocities of 8.1 km s^{-1}. The P wave velocities of the mantle below the Western Plateaus are slightly higher with 8.2 km s^{-1}. The crustal thickness of the Western Plateaus ranges between 9.3 km in the Samoan Basin to 17.2 km east of the Danger Island Troughs (Figs. 6 and 11).

5 Two different magmatic and tectonic regimes on the Manihiki Plateau

In general, the crust of the Manihiki Plateau is severely faulted due to the break-up of Ontong Java Nui "Super-LIP" (Chandler et al., 2012, 2013; Taylor, 2006). In previous works, the Western Plateaus was assumed to be of a similar structure as the High Plateau (Hussong et al., 1979; Viso et al., 2005) due to the lack of data from deep crustal layers. By interpreting our P and S wave velocity and gravity models along with the Poisson's ratio model, the crustal structure of the different sub-plateaus as well as their individual margins and adjacent ocean basins can be further constrained. Both sub-plateaus exhibit a HVZ in the lower crust. These HVZs with velocities higher than 7.1 km s^{-1} are also common at other oceanic LIPs (Coffin and Eldholm, 1994; Coffin et al., 2006; Richards et al., 2013; Ridley and Richards, 2010) and can be related to the presence of gabbros and the olivine and pyroxene fraction of primary magmas (Ridley and Richards, 2010) (Figs. 13 and 14). The crustal thicknesses of the Western Plateaus and the High Plateau differ. Whereas the High Plateau shows a constant crustal thickness of 20 km, which is comparable to other oceanic LIPs such as the Agulhas Plateau and southern Mozambique Ridge (Gohl and Uenzelmann-Neben, 2001; Gohl et al., 2011; Uenzelmann-Neben et al., 1999) with steep boundaries towards the adjacent oceanic basins, the Western Plateaus shows a gradual decrease in the crustal thick-

SED
6, 1863–1905, 2014

ness from 17.2 km in the east to 9 km in the west. A clear boundary between normal oceanic crust in the Tokelau Basin and the oceanic LIP cannot be identified.

The middle crust of both sub-plateaus shows similarities in the P and S wave velocity structure. The middle crust of the Western Plateaus has a velocity field, which is comparable to the lower-middle crust of the High Plateau. This velocity and density distribution can be associated with mafic intrusions (Christensen, 1996; Coffin et al., 2006; Richards et al., 2013; Ridley and Richards, 2010). On the High Plateau, the upper-middle crust shows a slightly different velocity field and a small decrease in density (Table 1). This transitional layer is not present in the Western Plateaus. Additionally, the middle crust underlying the central High Plateau exhibits three large areas of higher Poisson's ratio, which are correlated to former volcanic centers observed in the seismic reflection data (Fig. 10). Those "chimneys" mark former magmatic pathways towards the seafloor of the High Plateau, possibly during a later volcanic stage (Fig. 14) (Pietsch and Uenzelmann-Neben, 2014). Karlstrom and Richards (2011) published a model of LIP crustal magma transport, which indicates the formation of individual upward migrating sills during later stages of volcanic activity. Similar structures cannot be observed on the Western Plateaus.

The upper crust of the two sub-plateaus differs significantly. The High Plateau consists of countless volcanic centers, which are partly eroded and covered by volcaniclastic and pelagic sedimentary rocks (Ai et al., 2008; Beiersdorf et al., 1995b). Thus, the upper crust consists of basaltic flow units as well as mafic intrusions (Ito and Taira, 2000; Karlstrom and Richards, 2011), possibly interlayering each other as a result of the multiple stages of secondary volcanism. Massive fault systems are only present at the margins of the High Plateau (Fig. 14) (Pietsch and Uenzelmann-Neben, 2014). At the Manihiki Scarp, deeper crustal layers, most likely consistent with the lower-middle crust, crop out at the seafloor in multiple ridges separated by deep reaching faults. Based on gravity data Viso et al. (2005) postulated that the upper crust was serpentinized in this area. We can further support this assumption by high values in the Possion's ratio (Fig. 10) and lower densities (Fig. 12) at the Manihiki Scarp and the

Penrhyn Basin. The margins towards the Samoan Basin and the Samoan basin themselves show basaltic flow units and have no indications for large-scale serpentinization in this area.

Whereas the High Plateau shows clear indications for multiple volcanic phases within its upper crust, the data from the Western Plateaus presents possible basaltic flow units only in the Samoan Basin. The upper crust of the Western Plateaus is heavily structured by fault systems and horst and graben features (Fig. 13). *P* and *S* wave modeling as well as gravity anomaly modeling reveal the presence of diverse rock types. It can be debated whether the upper crust consists of volcaniclastic deposits or even massive carbonate banks (Grevemeyer et al., 2001). Volcanic structures comparable to the High Plateau are not visible in any used data set on the southern Western Plateaus. The majority of the faults are normal faults, which is consistent with crustal stretching processes. Another indicator for crustal extension is the constant decrease in Moho depth towards the Tokelau Basin. Therefore, tectonic deformation seems to have modified the plateau's structure enormously. Volcanic extrusions, e.g. the occurrence of seamounts, can only be interpreted for the Tokelau Basin and are not present on the Western Plateaus (Fig. 13), at least in the currently imaged area. The dominant features of the Western Plateaus are formed by sedimentary basins and horst and graben structures.

The Danger Island Troughs dissect the Manihiki Plateau into the two main subplateaus. The trough is characterized by the absence of typical upper crustal material (Fig. 13). The lower crustal layers as well as the crust-mantle boundary show only few relicts of a former spreading center at this position. In the middle crust, the Danger Island Troughs mark the distinct change over between a single layer middle crust on the Western Plateaus and the upper-middle crust and lower-middle crust of the High Plateau (Figs. 2b and 13). Thus, the Danger Island Troughs separates two structural regimes, the tectonically deformed Western Plateaus and the volcanically altered High Plateau.

6 Discussion: Western Plateaus vs. High Plateau – two different crustal environments of the Manihiki Plateau

This paper presents the first comprehensive insight into the crustal structure of the sub-plateaus of the Manihiki Plateau. The results of our analyses revise earlier models. The Western Plateaus and the High Plateaus of the Manihiki Plateau show amazing differences, especially in the upper crustal layers and the crustal thicknesses.

6.1 Comparison with other oceanic LIPs

By comparing the Western Plateaus and the High Plateau with other oceanic LIPs, the crustal thickness and velocity-depth distribution of the High Plateau resembles those of the Kerguelen Plateau (Charvis and Operto, 1999), Broken Ridge (Francis and Raitt, 1967), Agulhas Plateau (Gohl and Uenzelmann-Neben, 2001; Parsiegla et al., 2008) and Mozambique Ridge (Gohl et al., 2011) (Fig. 15). The proportional velocity-depth distribution is also similar to that of the southern Ontong Java Plateau (Miura et al., 2004), but the Ontong Java Plateau exhibits up to twice the crustal thickness.

A dominant feature of all oceanic LIPs is the HVZ of the lower crust with *P* wave velocities ranging between 7.7 and 7.1 $\mathrm{km\,s^{-1}}$ (Fig. 15) (Coffin et al., 2006; Ridley and Richards, 2010). Both the Western Plateaus and the High Plateau show such high *P* wave velocities in the lower crust. High velocities are also present in the lower middle crust (*P* wave velocities between 6.3 and 7.0 $\mathrm{km\,s^{-1}}$).

The High Plateau along with other oceanic LIPs has an upper middle crustal layer of *P* wave velocities around 6.0 $\mathrm{km\,s^{-1}}$. This layer is not resolved as a crustal unit in all LIPs, but in general is present as a part of the middle crust. Surprisingly, this transitional layer is not present on the Western Plateaus (Fig. 15). Therefore the Western Plateaus is missing a crustal layer present in all other oceanic LIPs, a layer associated with mafic intrusions formed during a secondary volcanic phase (Inoue et al., 2008; Karlstrom and Richards, 2011; Miura et al., 2004). In addition, the upper crust of the Western Plateaus consists of several areas of very low velocities and low rock densities that are associated with volcaniclastic sedimentation and carbonate banks rather than with igneous rocks (Grevemeyer et al., 2001). The upper crust of oceanic LIPs mainly consists of basaltic flow units interlayered with pillow lavas and possibly sedimentary layers formed by regional secondary volcanic phases (Inoue et al., 2008).

The High Plateau shows local volcanic centers, which have been the outlets of intrusive and extrusive magmatism during secondary volcanic phases, similar as observed on the Ontong Java Plateau (Inoue et al., 2008) or the Hikurangi Plateau (Davy and Wood, 1994; Davy et al., 2008; Hoernle et al., 2004). Extrusive and intrusive volcanic activity is also visible in seismic reflection data throughout the High Plateau (Pietsch and Uenzelmann-Neben, 2014). Buried seamount chains can also be located in gravity anomaly grids on the High Plateau of the Manihiki Plateau (Fig. 12). This seems not to be the case for the southern Western Plateaus. Neither the seismic refraction/wide-angle reflection data nor the multichannel seismic reflection data acquired on the Western Plateaus indicate extensive secondary volcanism. Gravity anomalies are mainly attributed to fault complexes and ridge systems (Fig. 11). This has so far not been reported for any oceanic LIP. Basaltic flow units cropping out at the seafloor are only present in the Tokelau Basin. Therefore, the Western Plateaus of the Manihiki Plateau do not have the typical crustal structure of an oceanic LIP and lack features such as mafic intrusions in the upper-middle crust and basaltic flow units within the upper crust (Fig. 15). The High Plateau does show all features previously described for oceanic LIPs. The two main sub-plateaus of the Manihiki Plateau hence must have undergone a different magmatic and tectonic evolution after their emplacement as part of Ontong Java Nui.

6.2 Emplacement scenario of the Manihiki Plateau and its two major sub-plateaus

The initial volcanic event of a LIP emplaces approximately 75 % of the total igneous volume of the igneous province (Bryan and Ernst, 2008; Karlstrom and Richards, 2011), therefore it is consistent that the lower crustal layers as well as the middle crustal lay-

SED
6, 1863–1905, 2014

ers show similar attributes on both sub-plateaus of the Manihiki Plateau. The lower crust and the lower middle crust were emplaced during the "Super-LIP" event creating Ontong Java Nui (Chandler et al., 2012, 2013; Taylor, 2006). A large part of this "Super-LIP" was presumably at subaerial level (Fig. 16). Therefore the former upper crustal layers and volcanic centers were likely subject to erosion.

Rifting of Ontong Java Nui followed this initial magmatic phase (Chandler et al., 2012, 2013; Hoernle et al., 2004, 2010; Taylor, 2006; Timm et al., 2011; Worthington et al., 2006) (Fig. 16). The Danger Island Troughs, which separate the High and the Western Plateaus, formed during this time (Ingle et al., 2007; Timm et al., 2011) along with several fault systems at the Western Plateaus initiating the break-up between the Ontong Java Plateau and the Manihiki Plateau at several locations (Fig. 13). The conjugate margin at the eastern Ontong Java Plateau shows indications for a thinned LIP crust (Gladczenko et al., 1997; Klosko et al., 2001; Richardson et al., 2000), which can be associated with the crustal stretching during the initial phase of Ontong Java Nui rifting. On the eastern margin of the Manihiki Plateau a massive north-south trending transform fault creates the Manihiki Scarp (Fig. 1) (Larson et al., 2002; Viso et al., 2005). To the south, the Hikurangi Plateau rifted from the High Plateau of the Manihiki Plateau by the development of the Osbourn Trough ocean spreading center (Billen and Stock, 2000; Davy et al., 2008; Worthington et al., 2006).

With the beginning of seafloor spreading in the Ellice Basin and separation of the Manihiki Plateau from the Ontong Java Plateau (Chandler et al., 2012; Taylor, 2006; Worthington et al., 2006), the Western Plateaus experienced less tectonic deformation. As faults from the deeper crust to the seafloor can be detected (Fig. 13), the crustal stretching forces have been present throughout the different stages of the evolution of the Western Plateaus.

Simultaneously, a secondary volcanic stage started resulting in seamount chain volcanism on the High Plateau (Fig. 16). The relicts of volcanic centers as well as the magmatic pathways within the crust are visible in our data. The secondary volcanism formed the upper crust of the Manihiki Plateau by intrusive and extrusive volcanism

SED
6, 1863–1905, 2014

mainly of tholeiitic composition (Clague, 1976; Hoernle et al., 2010; Ingle et al., 2007; Timm et al., 2011). In addition, volcanic islands on the High Plateau such as Manihiki Atoll and Rakahanga (Beiersdorf et al., 1995a) formed during this volcanic stage. At the Danger Island Troughs, alkaline lavas are emplaced (Ingle et al., 2007).

At the Western Plateaus, we could not identify any evidence for secondary volcanism such as basaltic flow units or former seamounts. Of course, upper crustal layers created during a second volcanic stage could have been eroded as they were close to the sea surface. In this case, erosion should have been very effective, and volcanic pathways should be visible in the middle crustal layers of the presented models. Also, the unusual low velocities of the acoustic basement infer that the Western Plateaus experienced volcaniclastic and carbonatic sedimentation (Fig. 13). As no rock samples from this area are available for ground-truthing, we rely only on the geophysical parameters. The source of the volcaniclastic sedimentation is located most likely on the High Plateau. Carbonatic sedimentation, e.g. the build-up of carbonate platforms, is also likely since the Manihiki Plateau still has been relatively close to the sea surface. It is also common, that carbonate platforms form on fault blocks created by rifting processes and are later on buried by sedimentation (Bosence, 2005). Since the upper crust, consisting of sedimentary rocks, thins towards the west, and volcanic rocks become present again, it is likely that this portion of the Western Plateaus had already subsided deeper and was farther away from the source region of volcaniclastic sedimentation. Therefore, the western Western Plateaus experienced less sedimentation, and mafic rocks are exposed in the upper crust.

During a later stage of secondary volcanism, the volcanic activity on the High Plateau has weakened and moved its activity center to the east, as eastern volcanic structures are better preserved, and early deformed sedimentary layers are visible in seismic reflection data (Ai et al., 2008; Pietsch and Uenzelmann-Neben, 2014) (Fig. 16). Older volcanic edifices are eroded, leading to an almost smooth acoustic basement in the seismic reflection data (Pietsch and Uenzelmann-Neben, 2014). The eroded material is partially deposited on the High Plateau, but also becomes reworked and integrated into

SED
6, 1863–1905, 2014

the magma surfacing at the Danger Island Troughs (Ingle et al., 2007). Here, tholeiitic basalts with a U-shaped incompatible element pattern and unusually low abundance of several elements are formed. Those basalts cannot be found anywhere else on the sampled Manihiki Plateau or the other parts of Ontong Java Nui. Ingle et al. (2007) propose a magma formation characterized by extensive melting of depleted mantle wedge material and mixed with volcaniclastic sediment, possibly originated from the High Plateau. On the Western Plateaus, faults can be observed up to the acoustic basement, which leads to the conclusion that crustal stretching was still present during late secondary volcanism along with further sedimentation.

After the last magmatic pulse ceased, further pelagic sedimentation covered the volcanic relicts and tectonic motion generated faults and ridges. The Manihiki Plateau subsided into the current water-depth of 2600 m for the High Plateau and 4000 to 3600 m for the Western Plateaus (Fig. 16).

In summary, the Manihiki Plateau experienced multiple stages of magmatic emplacement and tectonic deformation. The Western Plateaus was mainly a subject to the tectonic forces related to the break-up of Ontong Java Nui and the resulting stretching of the LIP's crust. The Western Plateaus was cut off from the magma supply initiating the secondary volcanic stages, which are present on the High Plateau, but also on the conjugate Ontong Java Plateau and Hikurangi Plateau (Hoernle et al., 2004, 2010; Mahoney and Spencer, 1991; Mahoney et al., 1993). The Danger Island Troughs form the prominent dissection between those two sub-plateaus and their different magmatic and tectonic evolution. Our data indicate the lack of upper crust, and lower crustal material crops out at the base of the highly sedimented trough. Deep reaching faults could have channelized and limited the magma supply to the Danger Island Troughs and the High Plateau. The source of the secondary volcanism on the rifted Ontong Java Nui is different on each sub-plateau, which indicates possible separation – spatially and petrologically – of the source.

SED
6, 1863–1905, 2014

The interplay between tectonic and magmatic overprint proves to be a crucial key aspect in understanding the crustal nature of the Manihiki Plateau and its role in the rifting of the “Super-LIP” Ontong Java Nui.

7 Conclusions

We present the first seismic refraction/wide-angle reflection models of the two main sub-plateaus – the Western Plateaus and the High Plateau – of the Manihiki Plateau. From this newly gained information on the crustal structure of the sub-plateaus, the tectonic and magmatic evolution of this oceanic LIP can be reconstructed.

The Western Plateaus have a crustal thickness between 9.3 km in highly stretched LIP crust in the west and 17.2 km in the east. The upper crust does not consist of mafic extrusives as expected for an oceanic LIP. The upper crust consists of highly compacted sediments in basins created by deep reaching faults. By comparison with other oceanic LIPs, it becomes obvious that the Western Plateaus did not experience secondary volcanic stages.

The High Plateau shows the standard crustal structure of an oceanic LIP with a crustal thickness of up to 20 km. In the upper crust former eruptive centers of a secondary volcanic stage are visible. The feeder system of the LIP is traceable in the middle and lower crust.

The Danger Island Troughs is the distinct border between the volcanically active High Plateau and the Western Plateaus, which did not experience any further volcanic alteration, at least in their southern parts.

Our models indicate that the Manihiki Plateau experienced a different tectonic and magmatic evolution after the emplacement as a part of Ontong Java Nui. Whereas the High Plateau underwent secondary volcanism, comparable to the Ontong Java Plateau and the Hikurangi Plateau, and limited tectonic forces at its margins, the Western Plateaus experienced crustal stretching and magmatic starvation. These new insights in the formation and evolution of the Manihiki Plateau infer that the different sub-plateaus of the Manihiki Plateau played a key role in the break-up of the "Super-LIP" Ontong Java Nui.

Acknowledgements. We thank Ernst Flüh and Jörg Bialas of GEOMAR for providing the OBS and OBH systems. We also thank Cpt. L. Mallon and his crew of R/V *Sonne* for their support and assistance during the cruise So-224. This project contributes to the Workpackage 3.2 of the AWI Research Programm PACES. This project has been funded through a grant by the German Federal Ministry of Education and Research (BMBF) under project number 03G0224A and by institutional resources of the AWI.

References

Ai, H.-A., Stock, J. M., Clayton, R., and Luyendyk, B.: Vertical tectonics of the High Plateau region, Manihiki Plateau, Western Pacific, from seismic stratigraphy, Mar. Geophys. Res., 29, 13–26, doi:10.1007/s11001-008-9042-0, 2008.

Beiersdorf, H., Bach, W., Duncan, R. A., Erzinger, J., and Weiss, W.: New evidence for the production of EM-type ocean island basalts and large volumes of volcaniclastites during the early history of the Manihiki Plateau, Mar. Geol., 122, 181–205, doi:10.1016/0025-3227(94)00107-V, 1995a.

Beiersdorf, H., Bickert, T., Cepek, P., Fenner, J., Petersen, N., Schönfeld, J., Weiss, W., and Won, M. Z.: High-resolution stratigraphy and the response of biota to Late Cenozoic environmental changes in the central equatorial Pacific Ocean (Manihiki Plateau), Mar. Geol., 125, 29–59, doi:10.1016/0025-3227(95)00021-P, 1995b.

Billen, M. I. and Stock, J.: Morphology and origin of the Osbourn Trough, J. Geophys. Res., 105, 13481–13489, doi:10.1029/2000JB900035, 2000.

Bosence, D.: A genetic classification of carbonate platforms based on their basinal and tectonic settings in the Cenozoic, Sediment. Geol., 175, 49–72, doi:10.1016/j.sedgeo.2004.12.030, 2005.

Bryan, S. E. and Ernst, R. E.: Revised definition of large igneous provinces (LIPs), Earth-Sci. Rev., 86, 175–202, doi:10.1016/j.earscirev.2007.08.008, 2008.

Bryan, S. E. and Ferrari, L.: Large igneous provinces and silicic large igneous provinces: progress in our understanding over the last 25 years, Geol. Soc. Am. Bull., 125, 1053–1078, doi:10.1130/B30820.1, 2013.

Chandler, M. T., Wessel, P., Taylor, B., Seton, M., Kim, S.-S., and Hyeong, K.: Reconstructing Ontong Java Nui: implications for Pacific absolute plate motion, hotspot drift and true polar wander, Earth Planet. Sc. Lett., 331–332, 140–151, doi:10.1016/j.epsl.2012.03.017, 2012.
Chandler, M. T., Wessel, P., and Sager, W. W.: Analysis of Ontong Java Plateau palaeolatitudes: evidence for large-scale rotation since 123 Ma?, Geophys. J. Int., 194, 18–29, doi:10.1093/gji/ggt075, 2013.
Charvis, P. and Operto, S.: Structure of the Cretaceous Kerguelen Volcanic Province (southern Indian Ocean) from wide-angle seismic data, J. Geodyn., 28, 51–71, doi:10.1016/S0264-3707(98)00029-5, 1999.
Christensen, N. I.: Poisson's ratio and crustal seismology, J. Geophys. Res., 101, 3139–3156, doi:10.1029/95JB03446, 1996.
Clague, D. A.: Petrology of basaltic and gabbroic rocks dredged from the Danger Island Troughs, Manihiki Plateau, Initial Rep. Deep Sea, 33, 891–911, 1976.
Coffin, M. F. and Eldholm, O.: Scratching the surface: estimating dimensions of large igneous provinces, Geology, 21, 515–518, doi:10.1130/0091-7613(1993)021<0515:STSEDO>2.3.CO;2, 1993.
Coffin, M. F. and Eldholm, O.: Large igneous provinces: crustal structure, dimensions, and external consequences, Rev. Geophys., 32, 1–36, doi:10.1029/93RG02508, 1994.
Coffin, M. F., Pringle, M. S., Duncan, R. A., Gladczenko, T. P., Storey, M., Müller, R. D., and Gahagan, L. M.: Kerguelen hotspot magma output since 130 Ma, J. Petrol., 43, 1121–1137, doi:10.1093/petrology/43.7.1121, 2002.
Coffin, M. F., Duncan, R. A., Eldholm, O., Fitton, J. G., Frey, F. A., Larsen, H. C., Mahoney, J. J., Saunders, A. D., Schlich, R., and Wallace, P. J.: Large igneous provinces and scientific ocean drilling: status quo and a look ahead, Oceanography, 19, 150–160, doi:10.5670/oceanog.2006.13, 2006.
Coulbourn, W. T., and Hill, P. J.: A field of volcanoes on the Manihiki Plateau: mud or lava?, Mar. Geol., 98, 367–388, doi:10.1016/0025-3227(91)90111-G, 1991.
Courtillot, V., Jaupart, C., Manighetti, I., Tapponnier, P., and Besse, J.: On causal links between flood basalts and continental breakup, Earth Planet. Sc. Lett., 166, 177–195, doi:10.1016/S0012-821X(98)00282-9, 1999.
Davy, B. and Wood, R.: Gravity and magnetic modelling of the Hikurangi Plateau, Mar. Geol., 118, 139–151, doi:10.1016/0025-3227(94)90117-1, 1994.

SED
6, 1863–1905, 2014

Davy, B., Hoernle, K., and Reinhard, W.: Hikurangi Plateau: crustal structure, rifted formation, and Gondwana subduction history, Geochem. Geophy. Geosy., 9, Q07004, doi:10.1029/2007GC001855, 2008.

Francis, T. J. G. and Raitt, R. W.: Seismic refraction measurements in the southern Indian Ocean, J. Geophys. Res., 72, 3015–3041, doi:10.1029/JZ072i012p03015, 1967.

Fromm, T.: AWIForge > Projects > PRay > Home, aforge.awi.de, available at: http://aforge.awi.de/gf/project/pray (last access: 22 January 2014), 2012.

Gladczenko, T. P., Coffin, M. F., and Eldholm, O.: Crustal structure of the Ontong Java Plateau: modeling of new gravity and existing seismic data, J. Geophys. Res., 102, 22711–22729, doi:10.1029/97JB01636, 1997.

Gohl, K. and Uenzelmann-Neben, G.: The crustal role of the Agulhas Plateau, southwest Indian Ocean: evidence from seismic profiling, Geophys. J. Int., 144, 632–646, doi:10.1046/j.1365-246X.2001.01368.x, 2001.

Gohl, K., Uenzelmann-Neben, G., and Grobys, N.: Groth and dispersal of a southeast African large igneous province, S. Afr. J. Geol., 114, 379–386, doi:10.2113/gssajg.114.3-4.379, 2011.

Grevemeyer, I., Weigel, W., Schüssler, S., and Avedik, F.: Crustal and upper mantle seismic structure and lithospheric flexure along the Society Island hotspot chain, Geophys. J. Int., 147, 123–140, doi:10.1046/j.0956-540x.2001.01521.x, 2001.

Hamilton, E. L.: Sound velocity–density relations in sea-floor sediments and rocks, J. Acoust. Soc. Am., 63, 366–377, doi:10.1121/1.381747, 1978.

Hoernle, K., Hauff, F., Reinhard, W., and Mortimer, N.: New insights into the origin and evolution of the Hikurangi oceanic plateau, Eos T. Am. Geophys. Un., 85, 401–408, doi:10.1029/2004EO410001, 2004.

Hoernle, K., Hauff, F., van den Bogaard, P., Reinhard, W., Mortimer, N., Geldmacher, J., Garbe-Schönberg, D., and Davy, B.: Age and geochemistry of volcanic rocks from the Hikurangi and Manihiki oceanic Plateaus, Geochim. Cosmochim. Ac., 74, 1–24, doi:10.1016/j.gca.2010.09.030, 2010.

Hussong, D. M., Wipperman, L. K., and Kroenke, L. W.: The crustal structure of the Ontong Java and Manihiki oceanic plateaus, J. Geophys. Res., 84, 6003–6010, doi:10.1029/JB084iB11p06003, 1979.

Ingle, S. P. and Coffin, M. F.: Impact origin for the greater Ontong Java Plateau?, Earth Planet. Sc. Lett., 218, 123–134, doi:10.1016/S0012-821X(03)00629-0, 2004.

Ingle, S. P., Mahoney, J. J., Sato, H., Coffin, M. F., Kimura, J.-I., Hirano, N., and Nakanishi, M.: Depleted mantle wedge and sediment fingerprint in unusual basalts from the Manihiki Plateau, central Pacific Ocean, Geology, 35, 595, doi:10.1130/G23741A.1, 2007.
Inoue, H., Coffin, M. F., Nakamura, Y., Mochizuki, K., and Kroenke, L. W.: Intrabasement reflections of the Ontong Java Plateau: implications for plateau construction, Geochem. Geophy. Geosy., 9, Q04014, doi:10.1029/2007GC001780, 2008.
Ito, G. and Taira, A.: Compensation of the Ontong Java Plateau by surface and subsurface loading, J. Geophys. Res., 105, 11171–11183, doi:10.1029/2000JB900036, 2000.
Karlstrom, L. and Richards, M. A.: On the evolution of large ultramafic magma chambers and timescales for flood basalt eruptions, J. Geophys. Res., 116, B08216, doi:10.1029/2010JB008159, 2011.
Klosko, E. R., Russo, R. M., Okal, E. A., and Richardson, W. P.: Evidence for a rheologically strong chemical mantle root beneath the Ontong–Java Plateau, Earth Planet. Sc. Lett., 186, 347–361, doi:10.1016/S0012-821X(01)00235-7, 2001.
Korenaga, J.: Why did not the Ontong Java Plateau form subaerially?, Earth Planet. Sc. Lett., 234, 385–399, doi:10.1016/j.epsl.2005.03.011, 2005.
Larson, R. L. and Erba, E.: Onset of the Mid-Cretaceous greenhouse in the Barremian-Aptian: igneous events and the biological, sedimentary, and geochemical responses, Paleoceanography, 14, 663–678, doi:10.1029/1999PA900040, 1999.
Larson, R. L., Pockalny, R. A., Viso, R. F., Erba, E., Abrams, L. J., Luyendyk, B., Stock, J. M., and Clayton, R.: Mid-Cretaceous tectonic evolution of the Tongareva triple junction in the southwestern Pacific Basin, Geology, 30, 67–70, doi:10.1130/0091-7613(2002)030<0067:MCTEOT>2.0.CO;2, 2002.
Mahoney, J. J. and Spencer, K. J.: Isotopic evidence for the origin of the Manihiki and Ontong Java oceanic plateaus, Earth Planet. Sc. Lett., 104, 196–210, doi:10.1016/0012-821X(91)90204-U, 1991.
Mahoney, J. J., Storey, M., Duncan, R. A., Spencer, K. J., and Pringle, M.: Geochemistry and geochronology of Leg 130 basement lavas: nature and origin of the Ontong Java Plateau, Proceedings of the Ocean Drilling Programm Scientific Results, 130, 3–22, 1993.
McNutt, M. K.: Another nail in the plume coffin?, Science, 313, 1394, doi:10.1126/science.1131298, 2006.
Miura, S., Suyehiro, K., Shinohara, M., Takahashi, N., Araki, E., and Taira, A.: Seismological structure and implications of collision between the Ontong Java Plateau and Solomon

SED
6, 1863–1905, 2014

Diverse crustal structure and magmatic evolution of the Manihiki Plateau

K. Hochmuth et al.

Island Arc from ocean bottom seismometer–airgun data, Tectonophysics, 389, 191–220, doi:10.1016/j.tecto.2003.09.029, 2004.
Parsiegla, N., Gohl, K., and Uenzelmann-Neben, G.: The Agulhas Plateau: structure and evolution of a large igneous province, Geophys. J. Int., 174, 336–350, doi:10.1111/j.1365-246X.2008.03808.x, 2008.
Pietsch, R. and Uenzelmann-Neben, G.: The Manihiki Plateau – a multistage volcanic emplacement history seen in high resolution seismic reflection data, Earth Planet. Sc. Lett., in preparation, 2014.
Richards, M. A., Contreras-Reyes, E., Lithgow-Bertelloni, C., Ghiorso, M., and Stixrude, L.: Petrological interpretation of deep crustal intrusive bodies beneath oceanic hotspot provinces, Geochem. Geophy. Geosy., 14, 604–619, doi:10.1029/2012GC004448, 2013.
Richardson, W. P., Okal, E. A., and Van der Lee, S.: Rayleigh–wave tomography of the Ontong–Java Plateau, Phys. Earth Planet. Int., 118, 29–51, doi:10.1016/S0031-9201(99)00122-3, 2000.
Ridley, V. A. and Richards, M. A.: Deep crustal structure beneath large igneous provinces and the petrologic evolution of flood basalts, Geochem. Geophy. Geosy., 11, Q09006, doi:10.1029/2009GC002935, 2010.
Sandwell, D. T. and Smith, W. H.: Marine gravity anomaly from Geosat and ERS 1 satellite altimetry, J. Geophys. Res., 102, 10039–10054, doi:10.1029/96JB03223, 1997.
Schlanger, S. O., Jackson, E., Boyce, R. E., Cook, H., Jenkyns, H. C., Johnson, D., Kaneps, A., Kelts, K., Martini, E., McNulty, C., and Winterer, E. L.: Inital Reports of the Deep Sea Drilling Project, 33, 1–354, 1976.
Tarduno, J. A.: Evidence for extreme climatic warmth from Late Cretaceous arctic vertebrates, Science, 282, 2241–2243, doi:10.1126/science.282.5397.2241, 1998.
Taylor, B.: The single largest oceanic plateau: Ontong Java–Manihiki–Hikurangi, Earth Planet. Sc. Lett., 241, 372–380, doi:10.1016/j.epsl.2005.11.049, 2006.
Timm, C., Hoernle, K., Reinhard, W., Hauff, F., van den Bogaard, P., Michael, P., Coffin, M. F., and Koppers, A. A. P.: Age and geochemistry of the oceanic Manihiki Plateau, SW Pacific: new evidence for a plume origin, Earth Planet. Sc. Lett., 304, 135–146, doi:10.1016/j.epsl.2011.01.025, 2011.
Uenzelmann-Neben, G.: The expedition of the research vessel "*Sonne*" to the Manihiki Plateau in 2012 (So 224), Reports of Polar and Marine Research, 2012.

Uenzelmann-Neben, G., Gohl, K., Ehrhardt, A., and Seargent, M.: Agulhas Plateau, SW Indian Ocean: new evidence for excessive volcanism, Geophys. Res. Lett., 26, 1941–1944, doi:10.1029/1999GL900391, 1999.

Viso, R. F., Larson, R. L., and Pockalny, R. A.: Tectonic evolution of the Pacific–Phoenix–Farallon triple junction in the South Pacific Ocean, Earth Planet. Sc. Lett., 233, 179–194, doi:10.1016/j.epsl.2005.02.004, 2005.

Werner, R., Nürnberg, D., and Hauff, F.: R/V *Sonne* Fahrtbericht/Cruise Report SO225, GEOMAR Reports, 1–176, 2013.

White, R. S. and McKenzie, D.: Mantle plumes and flood basalts, J. Geophys. Res., 100, 17543–17,585, doi:10.1029/95JB01585, 1995.

Wignall, P. B.: Large igneous provinces and mass extinctions, Earth-Sci. Rev., 53, 1–33, doi:10.1016/S0012-8252(00)00037-4, 2001.

Winterer, E. L., Lonsdale, P. L., Matthews, J. L., and Rosendahl, B. R.: Structure and acoustic stratigraphy of the Manihiki Plateau, Deep-Sea Res., 21, 793–813, doi:10.1029/JB084iB11p06003, 1974.

Worthington, T. J., Hekinian, R., Stoffers, P., Kuhn, T., and Hauff, F.: Osbourn Trough: structure, geochemistry and implications of a mid-Cretaceous paleospreading ridge in the South Pacific, Earth Planet. Sc. Lett., 245, 685–701, doi:10.1016/j.epsl.2006.03.018, 2006.

Zelt, B.: zp – Software for plotting & picking SEGY seismic refraction data, www.soest.hawaii.edu, available from: http://www.soest.hawaii.edu/users/bzelt/zp/zp.html (last access: 22 January 2014), 2004.

Zelt, C. A. and Smith, R. B.: Seismic traveltime inversion for 2-D crustal velocity structure, Geophys. J. Int., 108, 16–34, doi:10.1111/j.1365-246X.1992.tb00836.x, 1992.

SED
6, 1863–1905, 2014

Table 1. Rock densities [kg m^{-2}] (Hamilton, 1978) used for specific layers in the gravity anomaly model.

Layer	AWI-20120100	AWI-20120200
sediments	2050	2050
low velocity upper crust	2400	not present
upper crust	2650	2800
upper middle crust	2800	2900
middle crust	2900	not present
lower middle crust	2950	2950
lower crust	3130	3150
mantle	3300	3300

SED
6, 1863–1905, 2014

Diverse crustal structure and magmatic evolution of the Manihiki Plateau

K. Hochmuth et al.

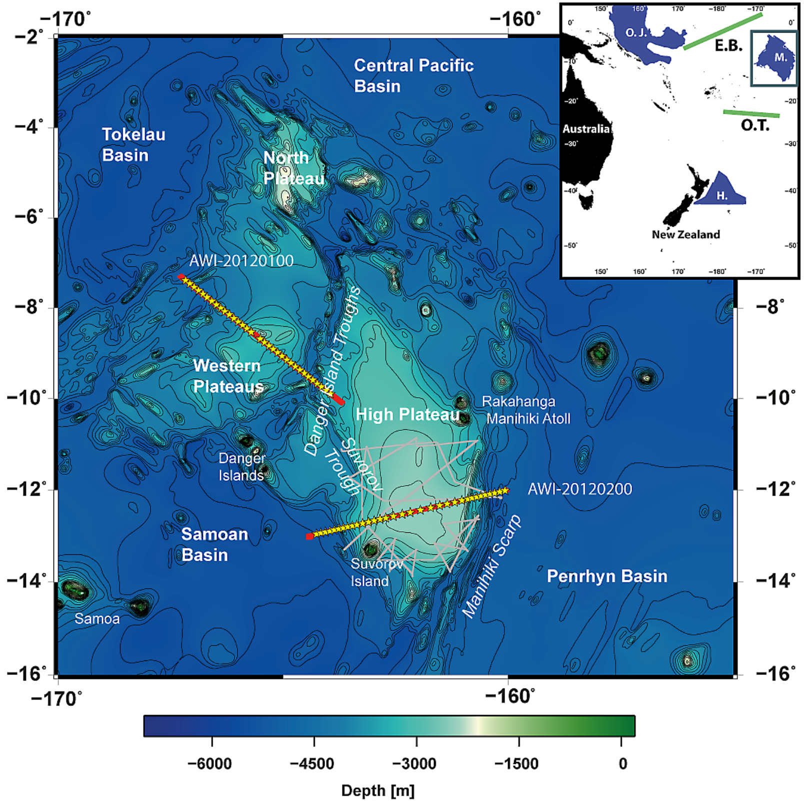

Figure 1. Bathymetric map of the central western Pacific, refraction/wide-angle refraction seismic lines of cruise So-224 are shown in red, reflection seismic lines of So-224 are shown in grey. Yellow stars depict the positions of the OBS-stations. In the inlet map the three main components of the Ontong Java Nui are shown at their current position (Ontong Java (O. J.), Hikurangi (H.) and Manihiki (M.)). The green lines indicate the former spreading centers of the Osbourn Trough (O. T.) and the Ellice Basin (E. B.). The dark green box indicates the study area shown in the larger map.

SED
6, 1863–1905, 2014

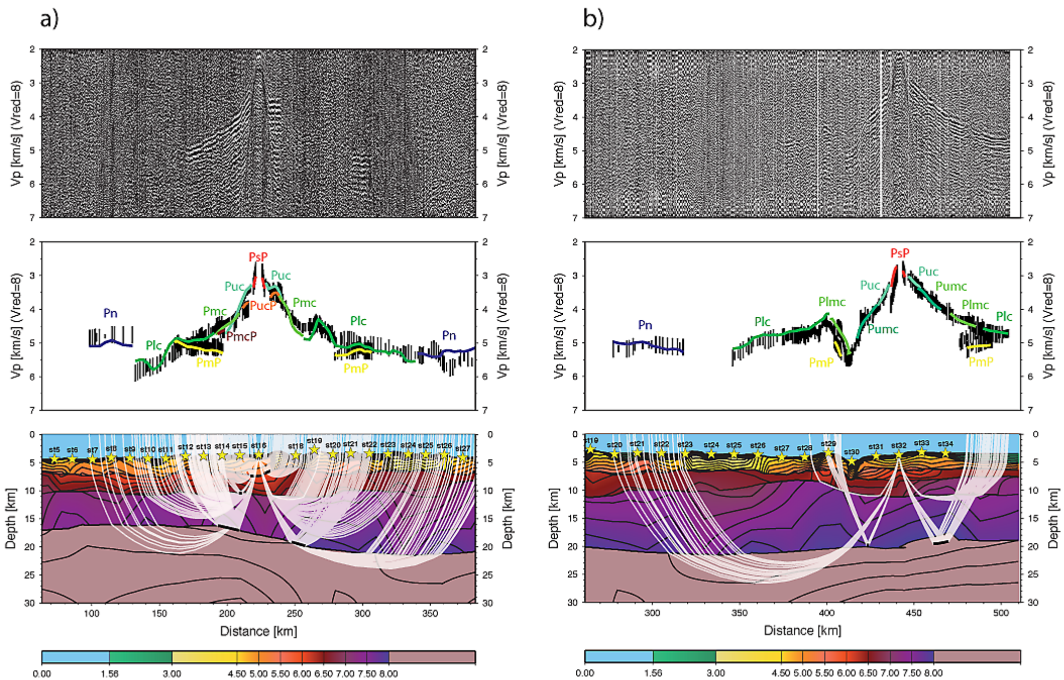

Figure 2. Data examples for *P* wave arrivals (AWI-20120100) at **(a)** st16 representing the central Western Plateaus and **(b)** st32 representing the Danger Island Troughs area.

SED
6, 1863–1905, 2014

Diverse crustal structure and magmatic evolution of the Manihiki Plateau

K. Hochmuth et al.

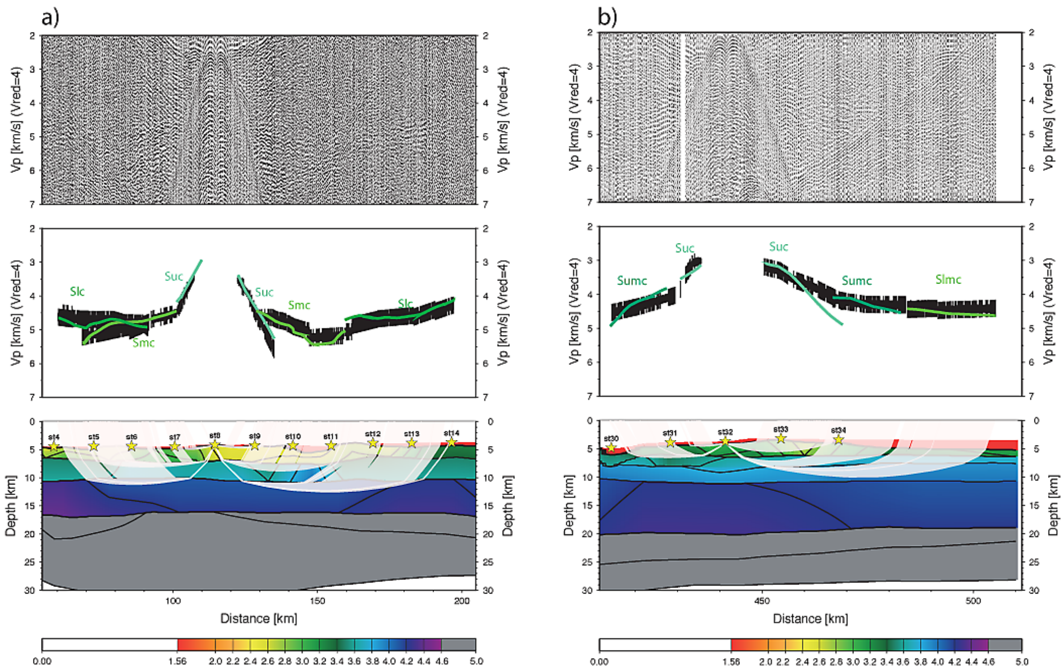

Figure 3. Data examples for *S* wave arrivals (AWI-20120100) at **(a)** st08 representing the western part of the Western Plateaus and **(b)** st32 representing the Danger Island Troughs area.

SED
6, 1863–1905, 2014

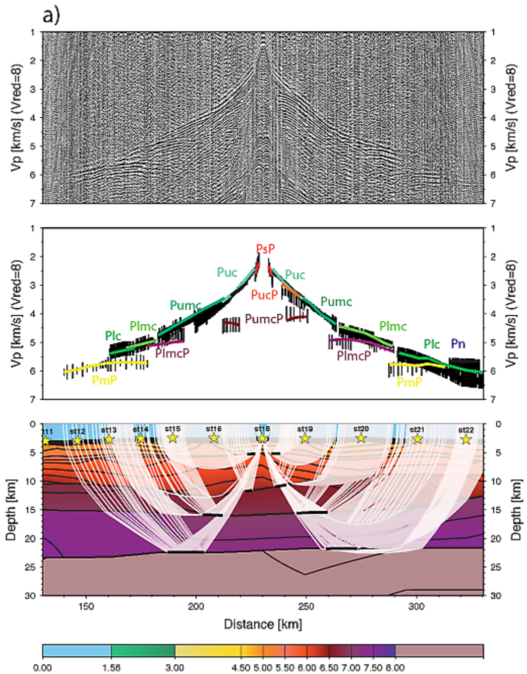

Figure 4. Data examples for *P* wave arrivals (AWI-20120200) at **(a)** st18 representing the central High Plateau and **(b)** st29 representing the Manihiki Scarp area.

SED
6, 1863–1905, 2014

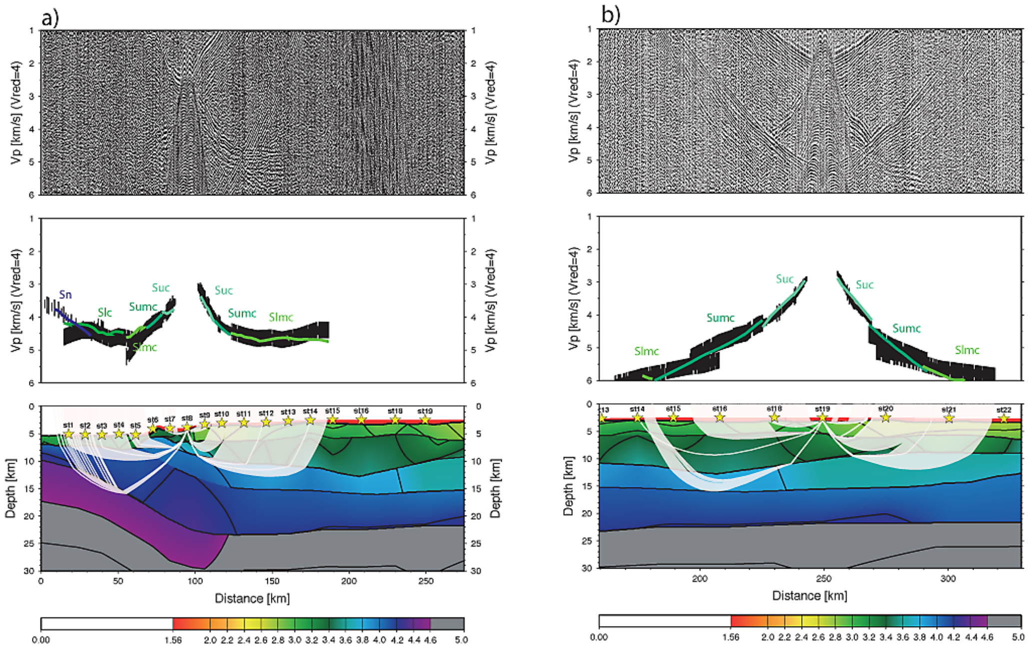

Figure 5. Data examples for *S* wave arrivals (AWI-20120200) at **(a)** st08 representing the western margin of the High Plateau and **(b)** st19 representing the central High Plateau.

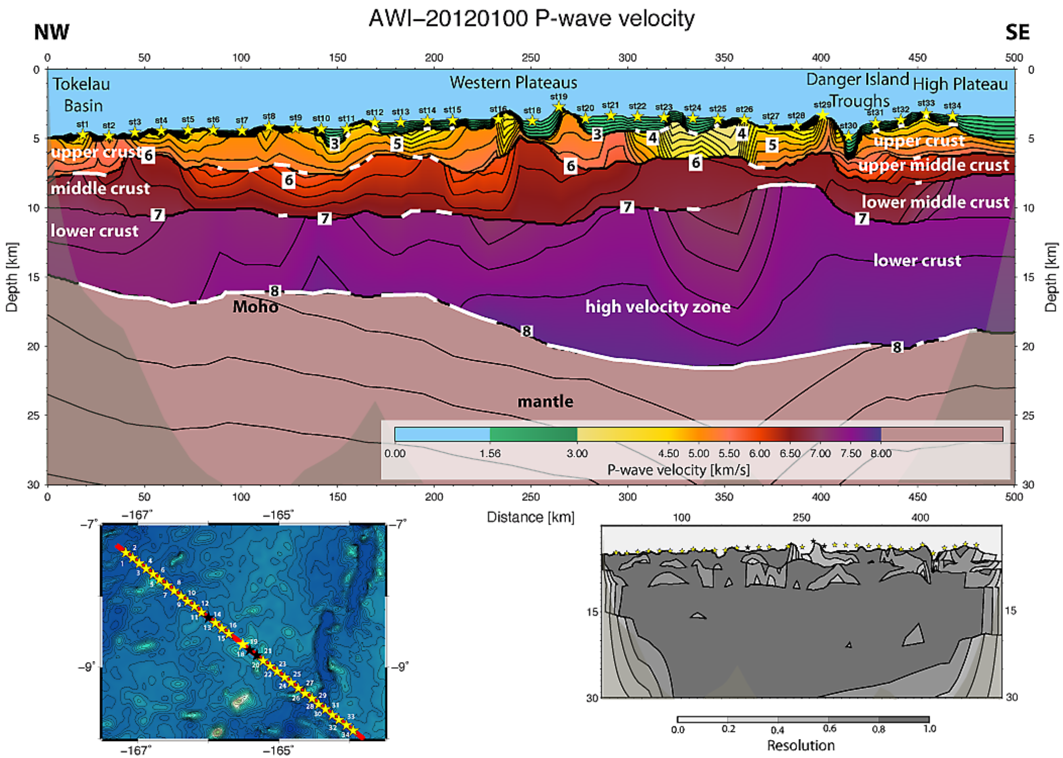

Figure 6. *P* wave velocity model of AWI-20120100; the grey transparent areas are not covered by rays. White layer boundaries are constraint by wide-angle reflections. The location of OBS stations is indicated with the yellow (functioning station) and black (malfunctioning station) stars on the map. The resolution calculated for the velocity nodes is shown in the lower right corner.

SED
6, 1863–1905, 2014

Diverse crustal structure and magmatic evolution of the Manihiki Plateau

K. Hochmuth et al.

Title Page
Abstract | Introduction
Conclusions | References
Tables | Figures
◄ | ►
◄ | ►
Back | Close
Full Screen / Esc
Printer-friendly Version
Interactive Discussion

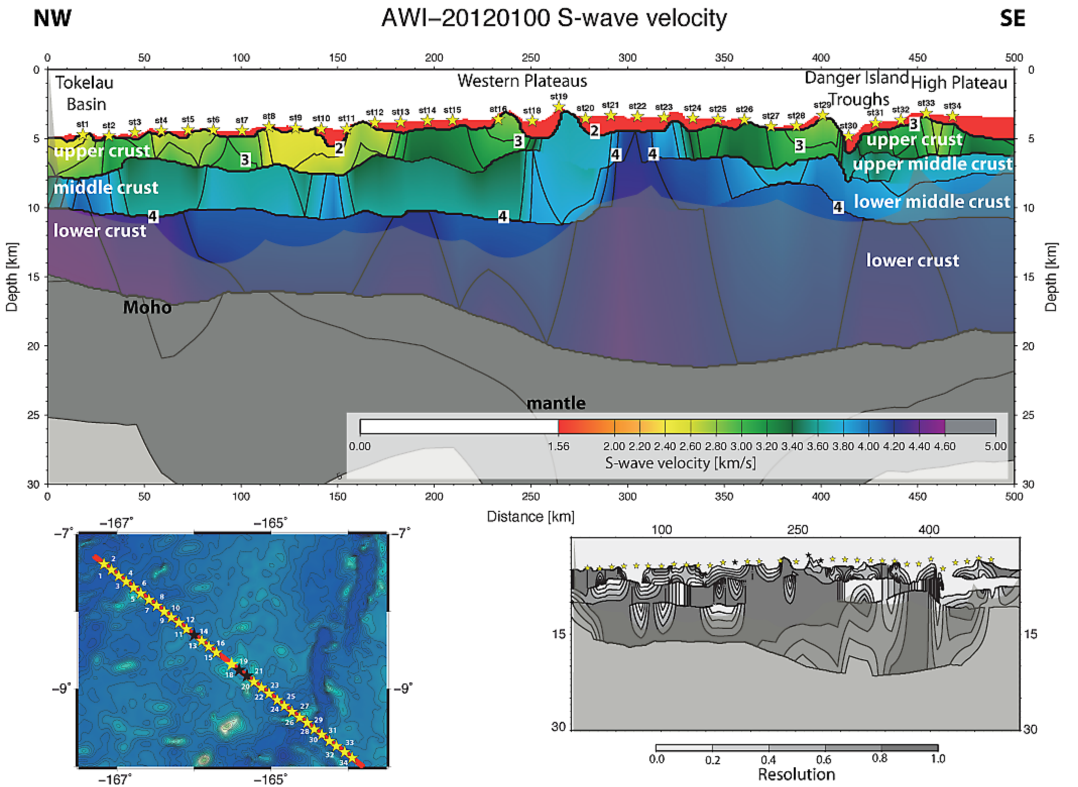

Figure 7. *S* wave velocity model of AWI-20120100; the grey transparent areas are not covered by rays. The locations of OBS stations are indicated with the yellow (functioning station) and black (malfunctioning station) stars on the map. The resolution calculated for the velocity nodes is shown in the lower right corner.

SED
6, 1863–1905, 2014

Diverse crustal structure and magmatic evolution of the Manihiki Plateau

K. Hochmuth et al.

Title Page
Abstract | Introduction
Conclusions | References
Tables | Figures
◀ | ▶
Back | Close
Full Screen / Esc
Printer-friendly Version
Interactive Discussion

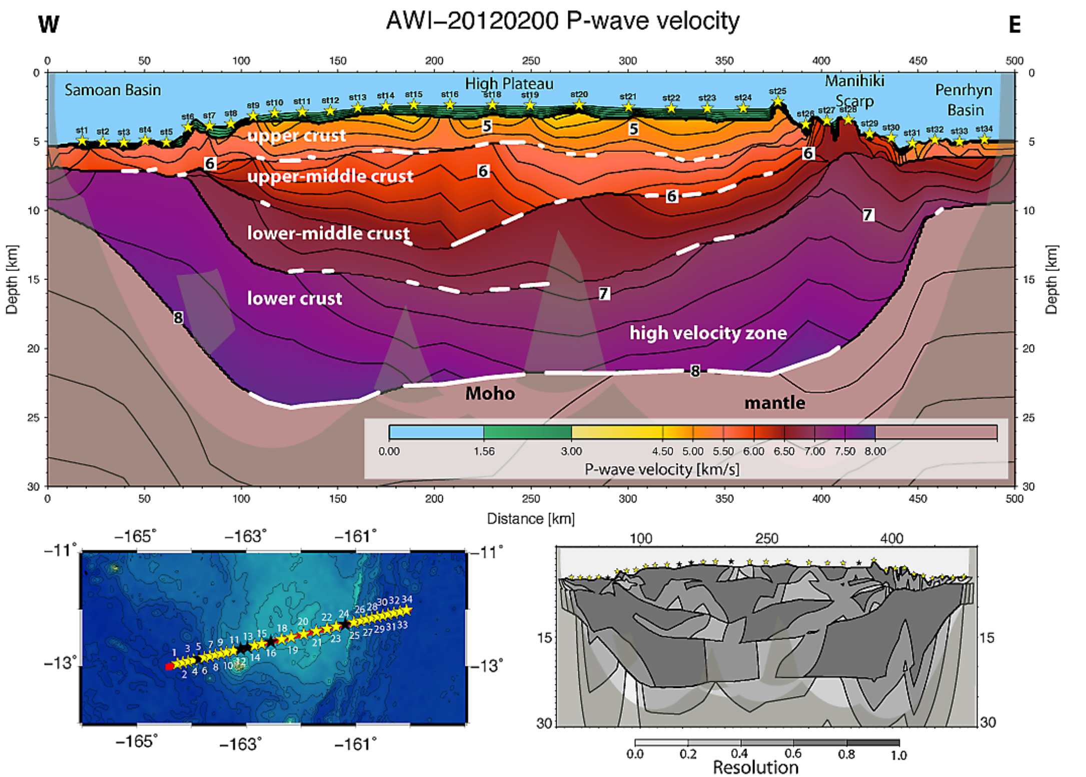

Figure 8. *P* wave velocity model of AWI-20120200; the grey transparent areas are not covered by rays. White layer boundaries are constrained by wide-angle reflections. The locations of OBS stations are indicated with the yellow (functioning station) and black (malfunctioning station) stars on the map. The resolution calculated for the velocity nodes is shown in the lower right corner.

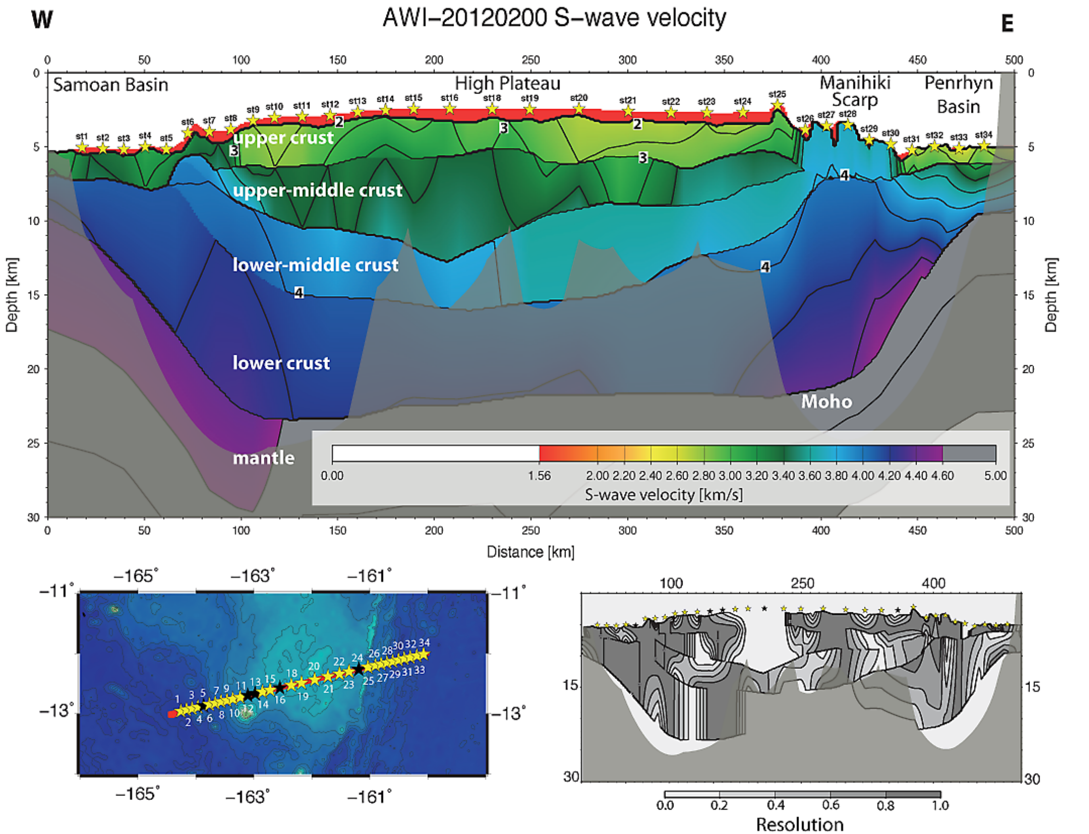

Figure 9. *S* wave velocity model of AWI-20120200; the grey transparent areas are not covered by rays. The locations of OBS stations are indicated with the yellow (functioning station) and black (malfunctioning station) stars on the map. The resolution calculated for the velocity nodes is shown in the lower right corner.

SED
6, 1863–1905, 2014

Diverse crustal structure and magmatic evolution of the Manihiki Plateau

K. Hochmuth et al.

Title Page
Abstract | Introduction
Conclusions | References
Tables | Figures
◂◂ | ▸▸
◂ | ▸
Back | Close
Full Screen / Esc
Printer-friendly Version
Interactive Discussion

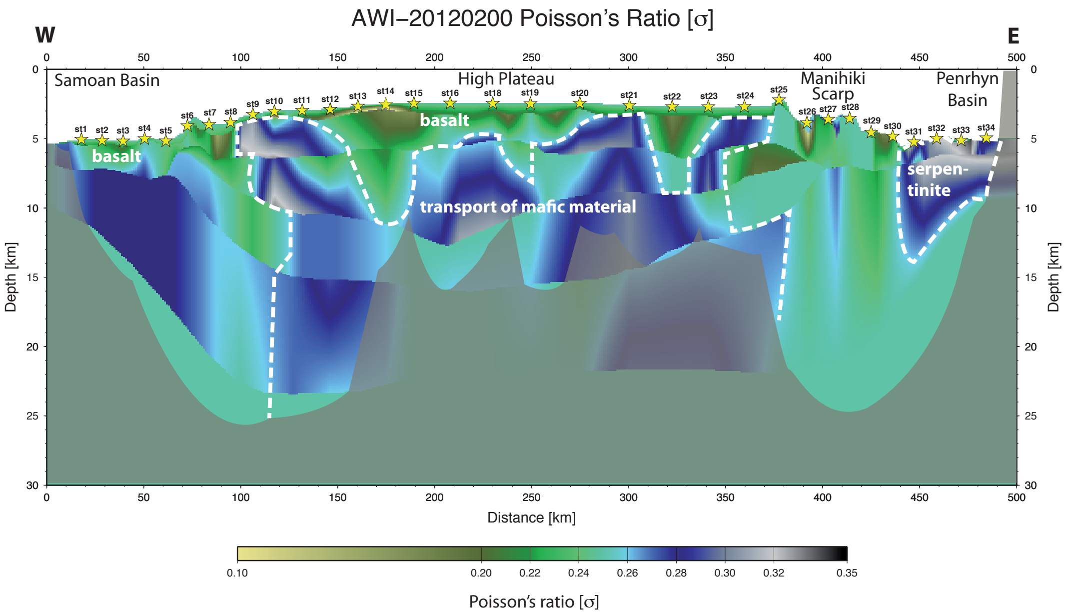

Figure 10. Calculated Poisson's ratio for AWI-20120200; grey shaded areas are not covered by rays in the *S* wave model and therefore cannot return reliable values for the Poisson's ratio. White dashed lines indicate areas of higher Poisson's ratio.

SED
6, 1863–1905, 2014

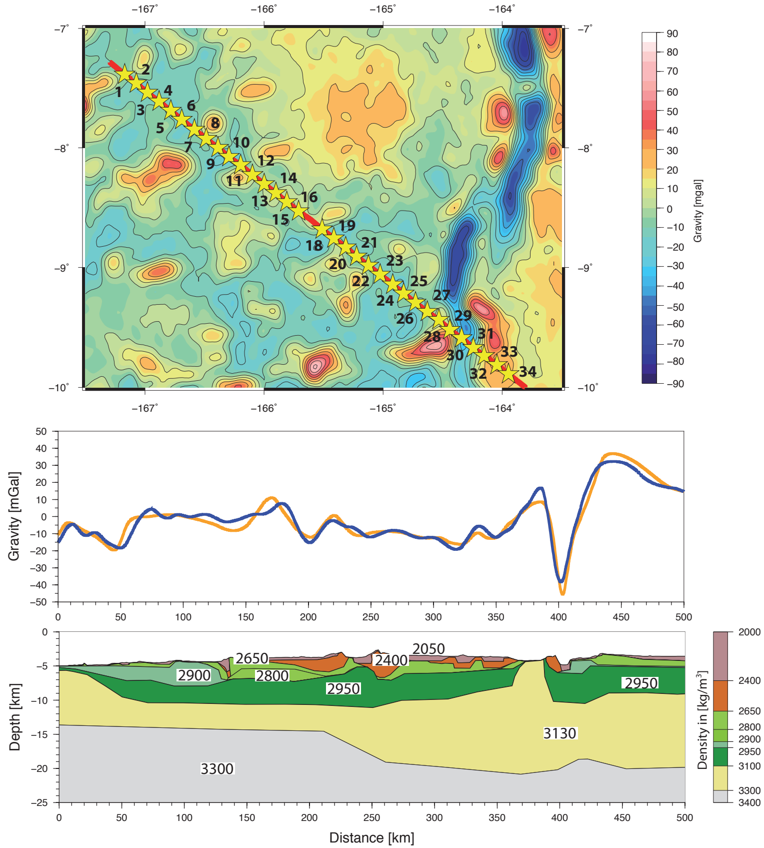

Figure 11. Gravity model of AWI-20120100 upper panel: freeair gravity anomaly (Sandwell and Smith, 1997) middle panel: measured anomaly in blue calculated anomaly in orange, lower panel: gravity model for AWI-20120100.

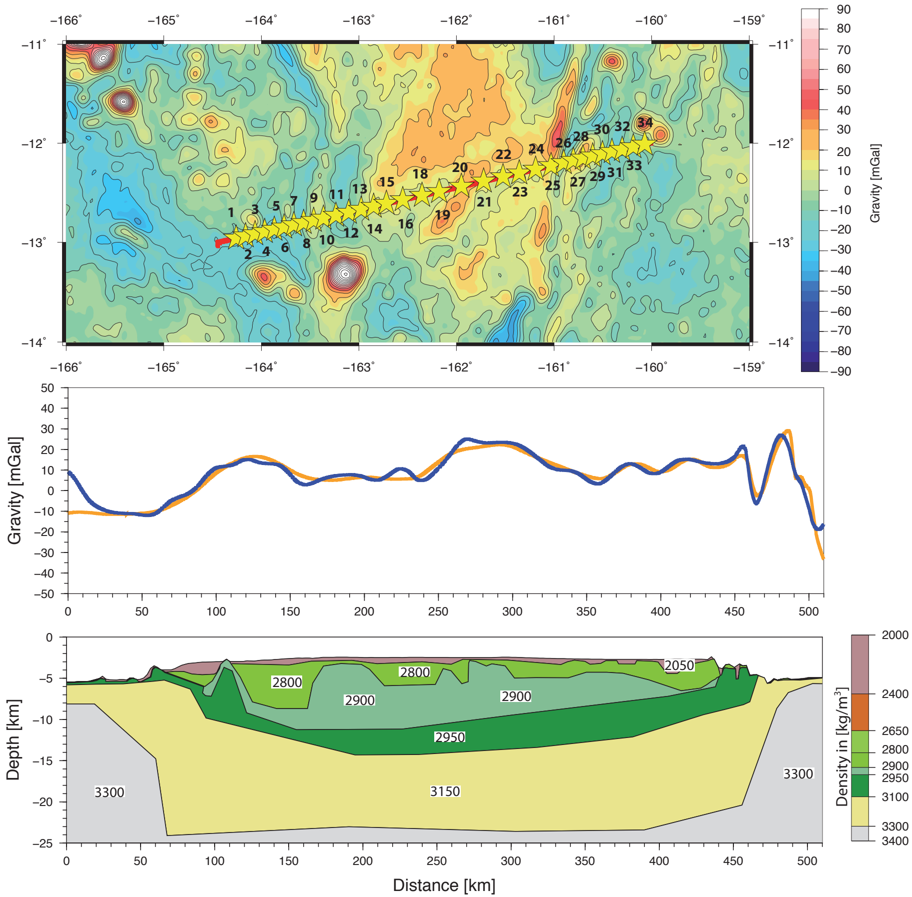

Figure 12. Gravity model of AWI-20120200 upper panel: free-air gravity anomaly (Sandwell and Smith, 1997) middle panel: measured anomaly in blue calculated anomaly in orange, lower panel: gravity model for AWI-20120200.

SED
6, 1863–1905, 2014

Diverse crustal structure and magmatic evolution of the Manihiki Plateau

K. Hochmuth et al.

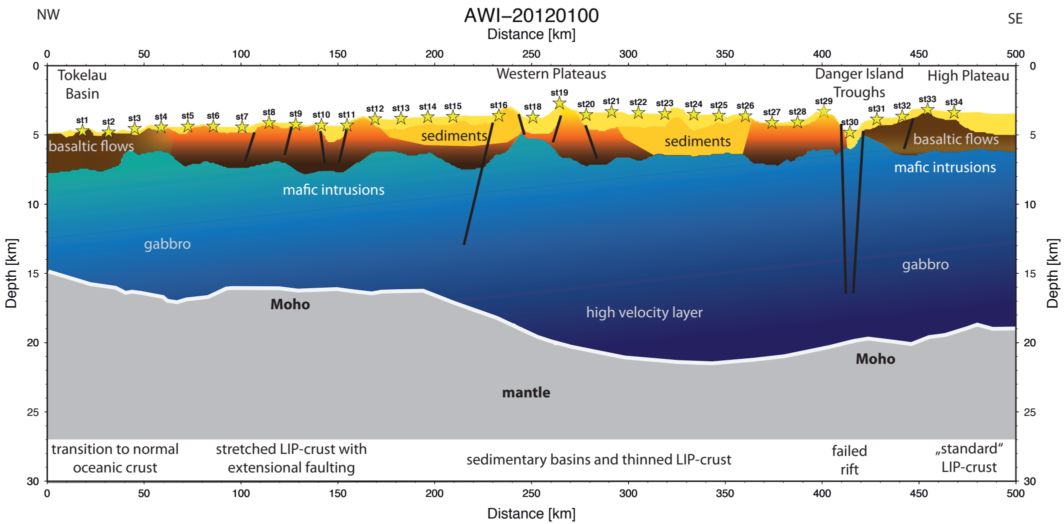

Figure 13. Sketch of geological interpretation of AWI-20120100, black lines indicate fault systems.

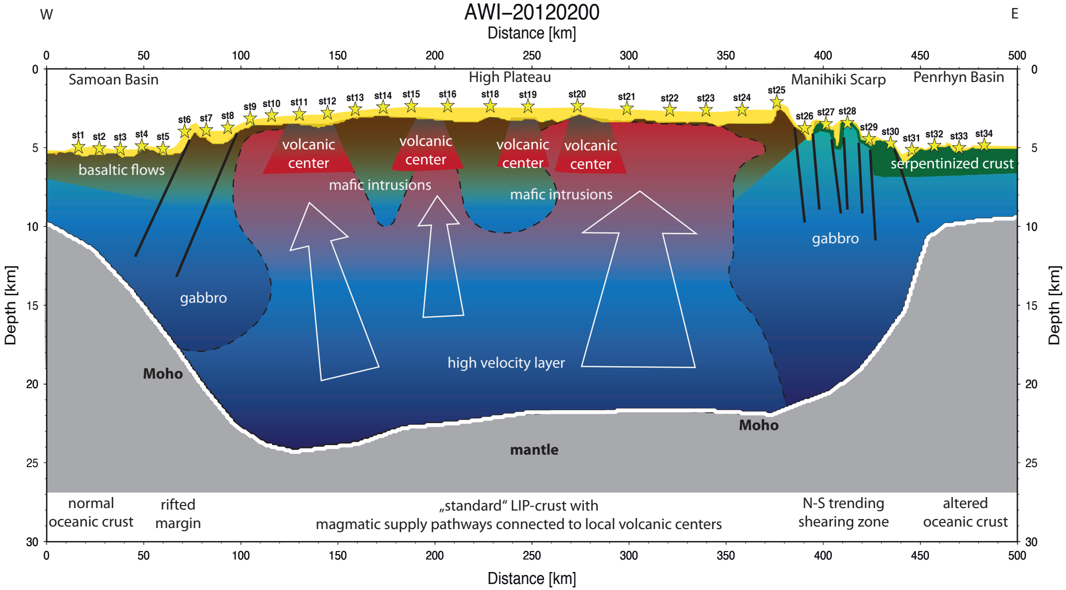

Figure 14. Sketch of geological interpretation of AWI-20120200, white arrows indicate areas of magmatic upwelling, black solid lines indicate fault systems.

SED
6, 1863–1905, 2014

Diverse crustal structure and magmatic evolution of the Manihiki Plateau

K. Hochmuth et al.

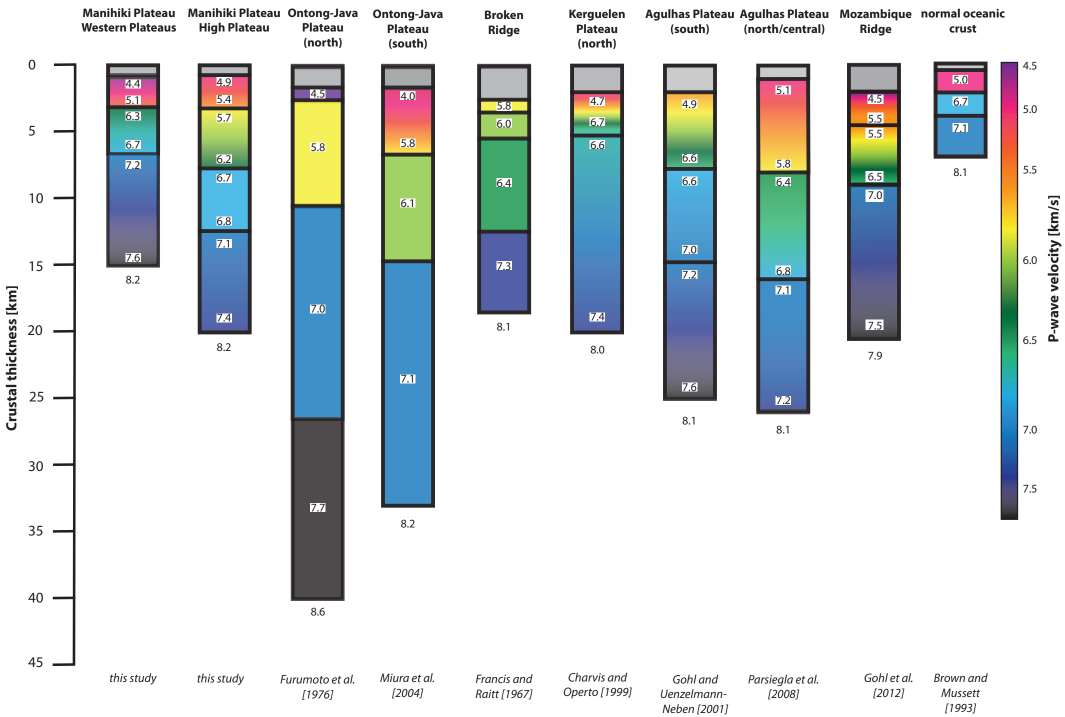

Figure 15. Comparison of the crustal structure of the Western Plateaus and the High Plateau with other oceanic LIPs. The grey shaded areas represent the sedimentary cover. The high velocity zone of the lower crust is represented in the blue colors. The transitional crustal layer is depicted in the yellow and orange colors.

Title Page
Abstract | Introduction
Conclusions | References
Tables | Figures
Back | Close
Full Screen / Esc
Printer-friendly Version
Interactive Discussion

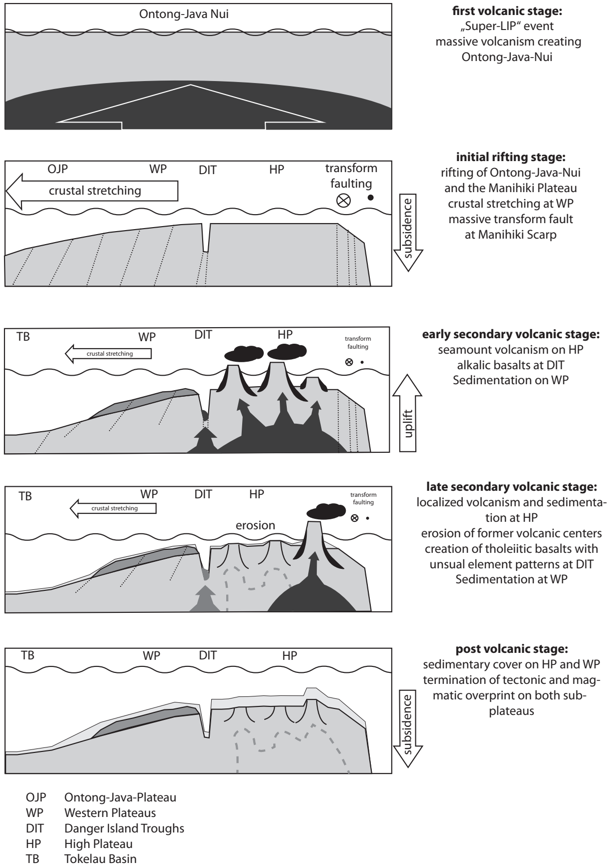

Figure 16. Sketch of the evolution of the Manihiki Plateau with special focus on the High Plateau and the Western Plateaus from the early Cretaceous to the current setting.